Parasitology

cambridge.org/par

Tankyrase inhibitors hinder *Trypanosoma cruzi* infection by altering host-cell signalling pathways

Laura Lafon-Hughes[1,2], Silvia H. Fernández Villamil[3,4] and Salomé C. Vilchez Larrea[3,5]

[1]Instituto de Investigaciones Biológicas Clemente Estable, Montevideo, Uruguay; [2]Grupo de Biofisicoquímica, Departamento de Ciencias Biológicas, Centro Universitario Regional Litoral Norte, Universidad de la República (CENUR-UdelaR), Salto, Uruguay; [3]Instituto de Investigaciones en Ingeniería Genética y Biología Molecular 'Dr. Héctor N. Torres', Consejo Nacional de Investigaciones Científicas y Técnicas, Ciudad Autónoma de Buenos Aires, Argentina; [4]Departamento de Química Biológica, Facultad de Farmacia y Bioquímica, Universidad de Buenos Aires, Ciudad Autónoma de Buenos Aires, Argentina and [5]Departamento de Fisiología, Biología Molecular y Celular, Facultad de Ciencias Exactas y Naturales, Universidad de Buenos Aires, Ciudad Autónoma de Buenos Aires, Argentina

Research Article

Cite this article: Lafon-Hughes L, Fernández Villamil SH, Vilchez Larrea SC (2021). Tankyrase inhibitors hinder *Trypanosoma cruzi* infection by altering host-cell signalling pathways. *Parasitology* **148**, 1680–1690. https://doi.org/10.1017/S0031182021001402

Received: 2 December 2020
Revised: 25 June 2021
Accepted: 28 July 2021
First published online: 12 August 2021

Key words:
Chagas disease; host–pathogen interaction; PARP; Tankyrase inhibitors; *Trypanosoma cruzi*; β-catenin signalling

Author for correspondence:
Salomé C. Vilchez Larrea,
E-mail: vilchez.ingebi@gmail.com;
Silvia H. Fernández Villamil,
E-mail: silvia.villamil@gmail.com

Abstract

Chagas disease is a potentially life-threatening protozoan infection affecting around 8 million people, for which only chemotherapies with limited efficacy and severe adverse secondary effects are available. The aetiological agent, *Trypanosoma cruzi*, displays varied cell invading tactics and triggers different host cell signals, including the Wnt/β-catenin pathway. Poly(ADP-ribose) (PAR) can be synthetized by certain members of the poly(ADP-ribose) polymerase (PARP) family: PARP-1/-2 and Tankyrases-1/2 (TNKS). PAR homoeostasis participates in the host cell response to *T. cruzi* infection and TNKS are involved in Wnt signalling, among other pathways. Therefore, we hypothesized that TNKS inhibitors (TNKSi) could hamper *T. cruzi* infection. We showed that five TNKSi (FLALL9, MN64, XAV939, G007LK and OULL9) diminished *T. cruzi* infection of Vero cells. As most TNKSi did not affect the viability of axenically cultivated parasites, our results suggested that TNKSi were interfering with parasite–host cell signalling. Infection by *T. cruzi* induced nuclear translocation of β-catenin, as well as upregulation of TNF-α expression and secretion. These changes were hampered by TNKSi. Further signals should be monitored in this model and *in vivo*. As a TNKSi has entered cancer clinical trials with promising results, our findings encourage further studies aiming at drug repurposing strategies.

Introduction

Chagas disease is an endemic Neglected Tropical Disease (NTD) in Latin America that affects an estimated 8 million people (https://www.who.int/chagas/epidemiology/en/) (Jansen *et al.*, 2018). The aetiological agent is *Trypanosoma cruzi*, a protozoan parasite that has a complex life cycle through which it alternates between an invertebrate insect vector and a mammalian host (Santi-Rocca *et al.*, 2017). The establishment of a successful infection relies on the interaction between the parasite and the mammalian host cell, which can be dissected into three steps: adhesion, signalling and invasion (de Souza *et al.*, 2010). After the initial binding and recognition of the parasite to the host cell, several signalling pathways are triggered in both parties to orchestrate the successful invasion, such as intracellular [Ca^{2+}] transients and PI3k/Akt signalling, among others (Burleigh and Woolsey, 2002; Woolsey *et al.*, 2003; Romano *et al.*, 2012). Wnt/β-catenin has been recently demonstrated to be one of these pathways, participating in the regulation of the inflammatory response and parasite intracellular replication (Volpini *et al.*, 2018).

Poly(ADP-ribose) (PAR) is synthetized by poly(ADP-ribose) polymerases (PARPs) as a post-translational protein modification mainly related to nuclear processes, although it has also been localized to extra-nuclear compartments (Lafon-Hughes *et al.*, 2014; Lafon Hughes *et al.*, 2017; Xie *et al.*, 2018). PAR homoeostasis has been implicated in the host cell response to *T. cruzi* infection (Vilchez Larrea *et al.*, 2012) as well as to other intracellular non-parasitic pathogens (Brady *et al.*, 2018; Miettinen *et al.*, 2019). During *T. cruzi* infection, host intracellular PAR levels raise both *in vivo* and *in vitro* (Wen *et al.*, 2018) and available evidence indicates that PARP-1 is crucial for the successful establishment of this parasitic infection: inhibition or silencing of PARP-1 in Vero and A549 cells leads to a marked decrease of infection levels *in vitro* (Vilchez Larrea *et al.*, 2012) and the absence of PARP-1 activity was proven beneficial for the maintenance of mitochondrial function in chagasic murine myocardium (Wen *et al.*, 2018).

Tankyrase-1 (TNKS-1) and Tankyrase-2 (TNKS-2) [telomeric repeat binding factor 1 (TRF1)-interacting ankyrin-related ADP-ribose polymerases], belong to the large PARP family and, like PARP-1 and PARP-2, are capable of synthesizing PAR in mammalian cells (Palazzo *et al.*, 2017; Lüscher *et al.*, 2018). Among other functions (Sbodio *et al.*, 2002; Hsiao and

CAMBRIDGE UNIVERSITY PRESS

Smith, 2008; De Boeck *et al.*, 2009), TNKS positively regulate Wnt/β-catenin signalling events: TNKS-mediated poly(ADP-ribosyl)ation (PARylation) of Axin (a scaffold protein in the β-catenin destruction complex) avoids β-catenin degradation, allowing its nuclear translocation (Yang *et al.*, 2016; Mariotti *et al.*, 2017). Wnt/β-catenin participation in the regulation of pro- and anti-inflammatory responses, mainly in cancer models, has drawn considerable attention in the past few years (Ma and Hottiger, 2016) and it has been reported that TNKS inhibitors (TNKSi) can modulate certain cytokine expression profiles (Levaot *et al.*, 2011).

Although the role of TNKS during viral cell infections has been explored in the past (Li *et al.*, 2012; Roy *et al.*, 2015), to our knowledge, the possible participation of host cell Tankyrases during *T. cruzi* or other parasitic infections and its modulation by TNKSi has never been explored. It was hypothesized that host cell Tankyrases could potentially affect *T. cruzi* infection by regulating the Wnt/β-catenin signalling pathway. We demonstrate that TNKSi were detrimental to *T. cruzi* infection in Vero cells but most did not affect parasite viability in axenic cultures. Host cell TNKS shifted towards the plasma membrane at early stages of infection (15 min). In response to *T. cruzi* infection in our model, β-catenin translocated to the nucleus (6 h post-infection) and the expression of the pro-inflammatory cytokine TNF-α was upregulated. TNKSi hindered these two responses, indicating that TNKS could be modulating *T. cruzi* cell infection through the regulation of these signalling molecules.

Materials and methods

Parasite and mammalian cells

Vero cells (ATCC® CCL-81™) were cultivated in MEM supplemented with 10% FCS, 100 U mL^{-1} penicillin, 0.1 mg mL^{-1} streptomycin and 2 mM glutamine. *Trypanosoma cruzi* parasites from the Tulahuen strain stably expressing the β-galactosidase gene (clone C4) (Buckner *et al.*, 1996) were maintained in culture by infection of Vero cells in MEM with 3% fetal bovine serum (FBS), 2 mM L-glutamine, 100 U mL^{-1} penicillin and 0.1 mg mL^{-1} streptomycin. *Trypanosoma cruzi* (Tulahuen strain) epimastigotes were cultured in Liver Infusion Tryptose (LIT) medium [5 g L^{-1} liver infusion, 5 g L^{-1} bacto-tryptose, 68 mM NaCl, 5.3 mM KCl, 22 mM Na_2HPO_4, 0.2% (W/V) glucose and 0.002% (W/V) hemin] supplemented with 10% FBS, 100 U mL^{-1} penicillin and 100 mg L^{-1} streptomycin for 7 days at 28°C.

Tankyrase inhibitors

XAV939 was purchased from Abcam (120897). All other inhibitors were kindly provided by Dr Lari Lehtiö (Biocenter Oulu, Faculty of Biochemistry and Molecular Medicine, University of Oulu, Finland). The reported potencies and IC_{50} are summarized in Table 1. The structure of the inhibitors is shown in Supplementary information Fig. S1.

β-Galactosidase infection assay

For the relative quantification of *T. cruzi* infection levels, the β-galactosidase expressing Tulahuen trypomastigotes were used. Vero cells were seeded in 96-well culture plates (10^4 cells/well in 100 μL MEM-10% FBS) and incubated ON. Then, trypomastigotes were added (MOI: 10:1) and washed after a 24 h incubation period. New culture media was added to infected monolayers, and 96 h after the addition of parasites to the culture (post-infection, p.i.), cell culture media was removed and cells and Tulahuen β-gal intracellular amastigotes were lysed in 100 μL lysis buffer (25 mM Tris pH 8, 2 mM EDTA, 2 mM DTT, 1% Triton X-100, 10% glycerol in ultrapure MQ water) for 10 min at 37°C. Then, 100 μL 2× reaction buffer [200 mM sodium phosphate pH 8, 2 mM MgCl2, 100 mM 2-mercaptoethanol and 1.33 mg mL^{-1} ortho-Nitrophenyl-β-galactoside (ONPG)] was added and the reaction was allowed to proceed until yellow colour developed (1–2 h at 37°C). Abs 420 nm was measured in a Synergy HTX multi-mode microplate reader (Biotek Instruments, Winooski, USA). Each infection condition or inhibitor was tested in triplicates and in four independent experiments. The absorbance at 420 nm obtained for each condition was normalized to the value obtained for the infection in the absence of inhibitors.

Viability of T. cruzi epimastigotes and extracellular amastigotes by Alamar blue

To evaluate the viability of *T. cruzi* epimastigotes or extracellular amastigotes, the Alamar blue method was used. Epimastigotes (5×10^6 parasites/well in LIT culture medium) were seeded in 96-well culture plates. TNKSi were added at the indicated concentrations and incubated for 96 h at 28°C. In the case of extracellular amastigotes, parasites were incubated in LIT medium in the presence of the drugs for 48 h, following the procedure reported by Takagi *et al.* (2019). After incubations, resazurin solution (final concentration 10 μg mL^{-1}) was added to each well and fluorescence was measured after 2 h in a Synergy HTX multi-mode microplate reader (Biotek Instruments, Winooski, USA) using the 530–560 nm emission and 590 nm excitation filters. Each condition was tested in triplicates and in at least three independent experiments.

Vero cell viability assessment by Alamar blue assay

Vero cells were seeded in 96-well culture plates (10^4 cells/well in 100 μL MEM-10% FBS). After 24 h, Tankyrase inhibitors were added to cell monolayers, incubated for 96 h and processed as described above. Each condition was tested in triplicates and in at least three independent experiments.

Trypomastigotes motility assessment

Trypomastigotes from the Tulahuen β-galactosidase strain obtained from the supernatant of infected Vero cell cultures were resuspended in fresh MEM-3% FBS to a concentration of 1×10^6 parasites mL^{-1} and incubated for 5 h at 37°C in the presence of TNKSi. After the incubation, motile parasites were counted under light microscope using a Neubauer chamber. The percentage of motile trypomastigotes was determined by considering the number of motile trypomastigotes at the start of the incubation as 100%. Each condition was tested in triplicates and in three independent experiments.

Immunocytofluorescence

Indirect immunocytofluorescence was carried as in Lafon-Hughes *et al.* (2014) (Lafon-Hughes *et al.*, 2014). Briefly, cells were seeded on glass coverslips in 24 well plates and subjected to the corresponding treatment or infection scheme. After fixation (PFA 4% β-catenin for or PFA 3%-glutaraldehyde 0.25% for TNKS), permeabilization and blocking, cells were incubated with 1:1000 anti-β-catenin (abcam 32572, Abcam, Cambridge, UK), 1:400 anti-TNKS (GTX117417, GeneTex, Irvine, CA, USA) or 1:500 anti-*T. cruzi* mouse serum, kindly provided by Dr Karina Gómez. After washing, samples were incubated with the correspondent secondary antibody (1 h, RT) and/or cytopainter (ab176756, Abcam, Cambridge, UK). Nuclei were counterstained

https://doi.org/10.1017/S0031182021001402 Published online by Cambridge University Press

Table 1. Potency of TNKS inhibitors towards PARP-1/2, TNKS-1/2 and TcPARP

PARP inhibitor	IC50 *in vitro* (nM)				
	PARP-1	PARP-2	TcPARP	TNKS-1	TNKS-2
FLALL 9 (compound 8)	>10 000 (Haikarainen *et al.*, 2013)	>10 000 (Haikarainen *et al.*, 2013)	–	5 (Haikarainen *et al.*, 2013)	>10 000 (Haikarainen *et al.*, 2013)
MN64	19 000 (Haikarainen *et al.*, 2014)	35 000 (Haikarainen *et al.*, 2014)	–	6 (Haikarainen *et al.*, 2014)	72 (Haikarainen *et al.*, 2014)
XAV 939	2200 (Riffell *et al.*, 2012; Lehtiö *et al.*, 2013), 5500 (Mariotti *et al.*, 2017), 74 (FL) (Thorsell *et al.*, 2017)	27 (Thorsell *et al.*, 2017) (FL)	1000: ≈40% inhibition (Vilchez Larrea *et al.*, 2012)	11–13 (Riffell *et al.*, 2012; Lehtiö *et al.*, 2013), 5 (Mariotti *et al.*, 2017), 95 (Thorsell *et al.*, 2017)	4–5 (Riffell *et al.*, 2012; Lehtiö *et al.*, 2013), 2 (Mariotti *et al.*, 2017), 5 (Thorsell *et al.*, 2017)
G007LK	–	–	–	46 (Haikarainen *et al.*, 2013)	25 (Haikarainen *et al.*, 2013)
OULL 9 (compound 6)	–	–	–	6300 (Nkizinkiko *et al.*, 2015)	300 (Nkizinkiko *et al.*, 2015)
OD35 (compound 2)	–	–	–	11 000 (Haikarainen *et al.*, 2016)	260 (Haikarainen *et al.*, 2016)

In vitro IC50 values determined for activity assays using full length (FL) or truncated recombinant enzymes. Dashes indicate information is not available.

with DAPI and coverslips were mounted in Prolong Gold (Molecular Probes P36930, Eugene, OR, USA).

To evaluate PAR formation in amastigotes and trypomastigotes, parasites were collected from the supernatant of infected cultures, treated with the indicated drug for 2 h and fixed with PFA 4%. After fixation, parasites were adhered to poly-lysine coated slides, permeabilized with PBS1x-Triton X-100 0.2% and blocked with PBS1x-Tween 0.05%-BSA 3%. Parasites were incubated with 1:100 PAR detecting reagent (MABE1031, Merck Millipore, Burlington, MA, USA) and 1:500 anti-*T. cruzi* mouse serum. After washing, samples were incubated with the correspondent secondary antibody (1 h, RT) and nuclei were counterstained with DAPI. Images were recorded with an Olympus BX61/FV300 (Tokyo, Japan) with a Plan Apo 60×/1.42 NA oil immersion objective microscope. Original images were taken in the same conditions as reference images of controls without primary antibodies at the same microscopy session. All images in each experimental series were taken with the same setting at the same confocal session. If modified, all were subjected to the same degree of brightness/contrast adjustment and Gaussian blur filtering, including the control without a primary antibody. The ImageJ free software (https://imagej.nih.gov/ij/download.html) was used for image processing.

Subcellular fractionation

Vero cell subcellular fractions at different times p.i. were obtained using two different commercial subcellular fractionation kits. For the obtention of nuclear, cytoplasmic, internal membrane and cytoplasmic membrane fractions in TNKS localization experiments, the Plasma Membrane Protein Extraction kit (101Bio, Mountain View, CA, USA, cat# P503) was used, following the manufacturer's instructions. For the obtention of nuclear, cytoplasmic and cell membrane fractions in β-catenin relocalization experiments, the ProteoJET kit (Fermentas, Vilnius, Lithuania, cat# K0311) was used, following the manufacturer's instructions. Three independent experiments were performed.

Epimastigote protein extraction

Epimastigotes were cultured in LIT media to a $1–2 \times 10^7$ parasites mL^{-1} density. Parasites were collected by centrifugation and resuspended in lysis buffer (10 mM HEPES, pH 7.9, 10 mM KCl, 0.1 mM EDTA, 0.1 mM EGTA, 1 mM dithiothreitol, 0.5 mM phenylmethylsulfonyl fluoride) after which they were sonicated (1 pulse 5 s) to complete lysis. Protein concentration was determined by Bradford.

Western blot

Total protein extracts (30 μg per lane) were subjected to 10% SDS-PAGE. Proteins were blotted onto nitrocellulose membranes by semi-dry transfer and membranes were blocked and incubated with corresponding primary antibody overnight at 4°C, followed by incubation for 1 h (RT) with secondary antibody diluted in the same buffer. Western blots were developed using the Western Lightning Plus ECL Substrate (Perkin Elmer, Waltham, MA, USA) and images were taken using the GeneGnome XRQ Chemiluminescence imaging system (Syngene, Cambridge, UK). The antibodies used were: 1:2000 anti-TNKS (GTX117417, GeneTex, Irvine, CA, USA), 1:2000 anti-Lamin A/C (STJ93885, St John's Laboratory, London, UK), 1:2000 CALR3 (STJ190646, St John's Laboratory, London, UK), 1:5000 anti-PMCA (kindly gifted by Dr Gerardo Corradi, IQUIFIB-CONICET, Buenos Aires, Argentina), 1:6000 anti-β-catenin (ab3572, Abcam, Cambridge, UK), 1:1000 anti-CyclinD1 (sc-718, Santa Cruz Biotechnologies, Dallas, TX, USA), 1:1000 anti-c-Myc (sc-764, Santa Cruz Biotechnologies, Dallas, TX, USA). For PAR detection, the pan-PAR-detecting reagent MABE 1031 (Merck Millipore, Burlington, MA, USA) was used (1:4000).

TNF-α expression quantification by RT-qPCR

Total RNA was extracted from Vero cells at 0 or 24 h p.i., in the presence or absence of 0.6 μM MN64 using Quick-zol reagent (Kalium Technologies, Bernal, Buenos Aires, Argentina), following the manufacturer's instructions. The integrity of the extracted RNA was evaluated by agarose gel electrophoresis and the amount of RNA was quantified by measuring absorbance at Abs 280 nm, using DS-11 Spectrophotometer (DeNovix, Wilmington, USA). cDNA was generated using the EasyScript Reverse Transcriptase kit (Transgen Biotech, Beijing, China). Gene expression was evaluated by real-time PCR using Mezcla Real-qPCR kit (Biodynamics, Buenos Aires, Argentina) in a RotorGene 6000

https://doi.org/10.1017/S0031182021001402 Published online by Cambridge University Press

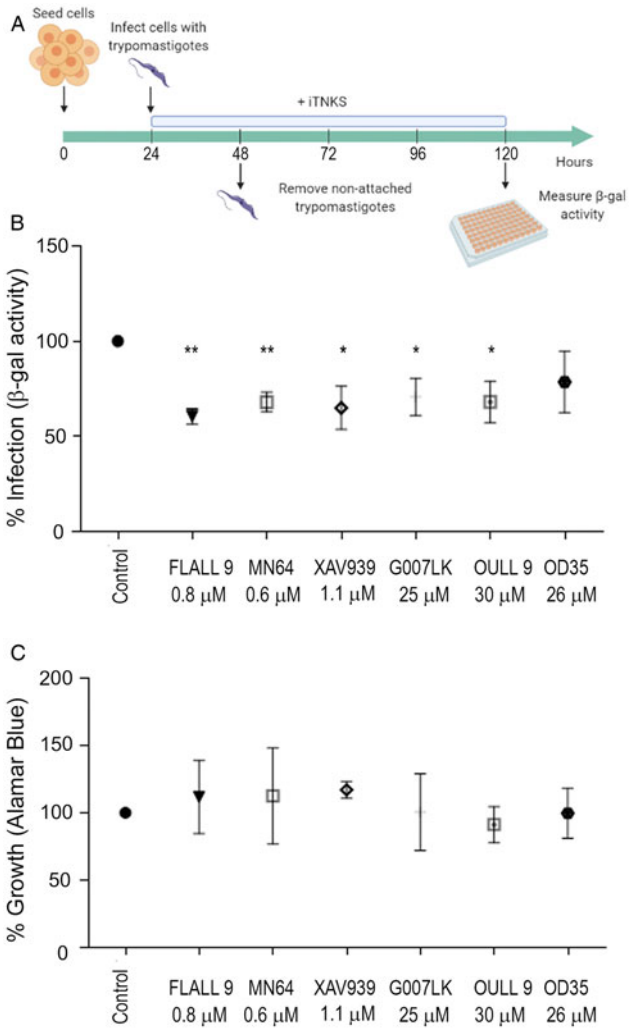

Fig. 1. TNKS inhibitors diminished *T. cruzi* Tul *β*-gal infection in Vero cells without affecting host cells viability. (A) Experimental schedule. Vero cells were seeded and infected the following day (MOI: 10:1) in the presence of the indicated concentrations of TNKSi. After 24 h, parasites were removed and fresh medium with TNKSi was added. (B) Amastigote load in Vero cells was quantified 144 h after cell seeding (96 h p.i.) by *β*-gal activity assay and expressed as % control infection. Mean ± standard error is shown. Data are from four independent experiments in triplicate. (C) The effect of TNKSi on uninfected Vero cell viability after 96 h was quantified by Alamar blue assay. Mean ± standard error is shown. Data are from three independent experiments in triplicate. *$P < 0.05$, **$P < 0.01$ according to one-way ANOVA and Fisher's LSD test.

(Corbett, Germantown, USA). The primers used were *Tnfa* 5′-TCCCTCTTCAAGGGCCAAGG-3′(Forward) and 5′-TGGG CTCATACCAGGGCTTG-3′(Reverse); *gapdh* 5′-CCTCCTG CACCACCAACTGC-3′(Forward) and 5′-TTCTGGGTGGCAGT GATGGC-3′(Reverse). Cycling conditions were: 95°C for 10 min, followed by 40 cycles of 95°C 15 s, 54°C 30 s for *Tnfa* and 58°C 30 sec for *gapdh*, and 72°C 15 s. Expression was normalized to the GAPDH (*gapdh*) and expressed in relation to control conditions in the absence of infection. Specificity was verified by performing melting curves after each amplification.

TNF- α capture ELISA

Vero cells were seeded in six-well plates and infected with *T. cruzi* Tulahuen trypomastigotes, in the presence or absence of XAV939 1.1 μM. Supernatants were collected 24 h p.i., centrifuged briefly to remove trypomastigotes, and analysed for TNF-α by capture ELISA using the OptEIA™ Human TNF ELISA Set (BD, San Diego, CA, USA, cat 555212), following the manufacturer's instructions. Quantification of TNF-α was performed by comparison against a recombinant hTNF-α standard curve.

Statistical analyses

The values obtained for the β-galactosidase infection experiments, viability determinations by Alamar blue, PAR staining, β-catenin nuclear staining, cMyc and Cyclin D1 Western blot band intensity quantification, qRT-PCR and colorimetric capture ELISA were compared by using Student's *t*-test or a one-way ANOVA when more than two means were considered. Calculations were carried out using GraphPad Prism.

Results

Tankyrase inhibitors diminished T. cruzi *infection in Vero cells in vitro without affecting host cell viability*

As a first approach to test the possible participation of host cell Tankyrases in *T. cruzi* infection, the effect of a panel of six TNKSi (see Fig. S1 for structures) was evaluated on *T. cruzi* infection in Vero cells, according to the experimental schedule displayed in Fig. 1A. The inhibitors were tested at concentrations corresponding to 100× the *in vitro* IC_{50} reported values (Table 1) (Fig. 1B).

Five out of the six inhibitors tested showed statistically significant decreases in the infection levels as measured by β-galactosidase activity at ~100×IC_{50} concentration (Fig. 1B). The largest effect was exerted by 0.8 μM FLALL 9, which reduced infection by 39.49% compared to the infection in the absence of any compound. The rest of the drugs diminished the infection by around 30% (MN64: 32.01%, XAV 939: 35.01%, G007LK: 29.24% and OULL 9: 31.98%).

The number of cell-associated parasites was also quantified at 1 h p.i. on Vero cell monolayers that were pre-treated with 0.8 μM FLALL 9 or 0.6 μM MN64, as indicated in the experimental schedule in Fig. S2A. In these experiments, TNKSi were removed prior to the addition of *T. cruzi* trypomastigotes. Infected or uninfected Vero cell monolayers were thoroughly washed, fixed and stained using an anti-*T. cruzi* serum to detect trypomastigotes, which were counted under the fluorescence microscope. The number of cell-associated parasites was significantly diminished (43.96% reduction) in the presence of MN64 (Fig. S2B). The addition of FLALL 9 also caused a slight decrease (21.66%) in the amount of *T. cruzi* parasites adhered to and/or internalized in Vero cells, but the difference was not significant.

The observed reduction in the infection levels could be due to a decrease in the trypomastigote invasion and/or amastigote replication success but could also be explained by the loss of viable cells in the culture. To test the latter scenario, the possible toxicity of these compounds on uninfected Vero cells was evaluated using the Alamar blue method. None of the compounds at the concentrations here tested affected the growth or viability of Vero cells in our experimental conditions. Concentrations above 100 × IC_{50}, however, reduced the viability of host cells in our model and were therefore not used for further experiments. These results indicated that the observed decrease in the infection levels at the concentrations previously tested could not be attributed to a reduction in host cell viability (Fig. 1C).

Tankyrase inhibitors did not hamper PAR synthesis in T. cruzi *nor affect parasites viability*

Next, it was evaluated if TNKSi were mitigating the infection of Vero cells by directly targeting the parasites or if the observed

https://doi.org/10.1017/S0031182021001402 Published online by Cambridge University Press

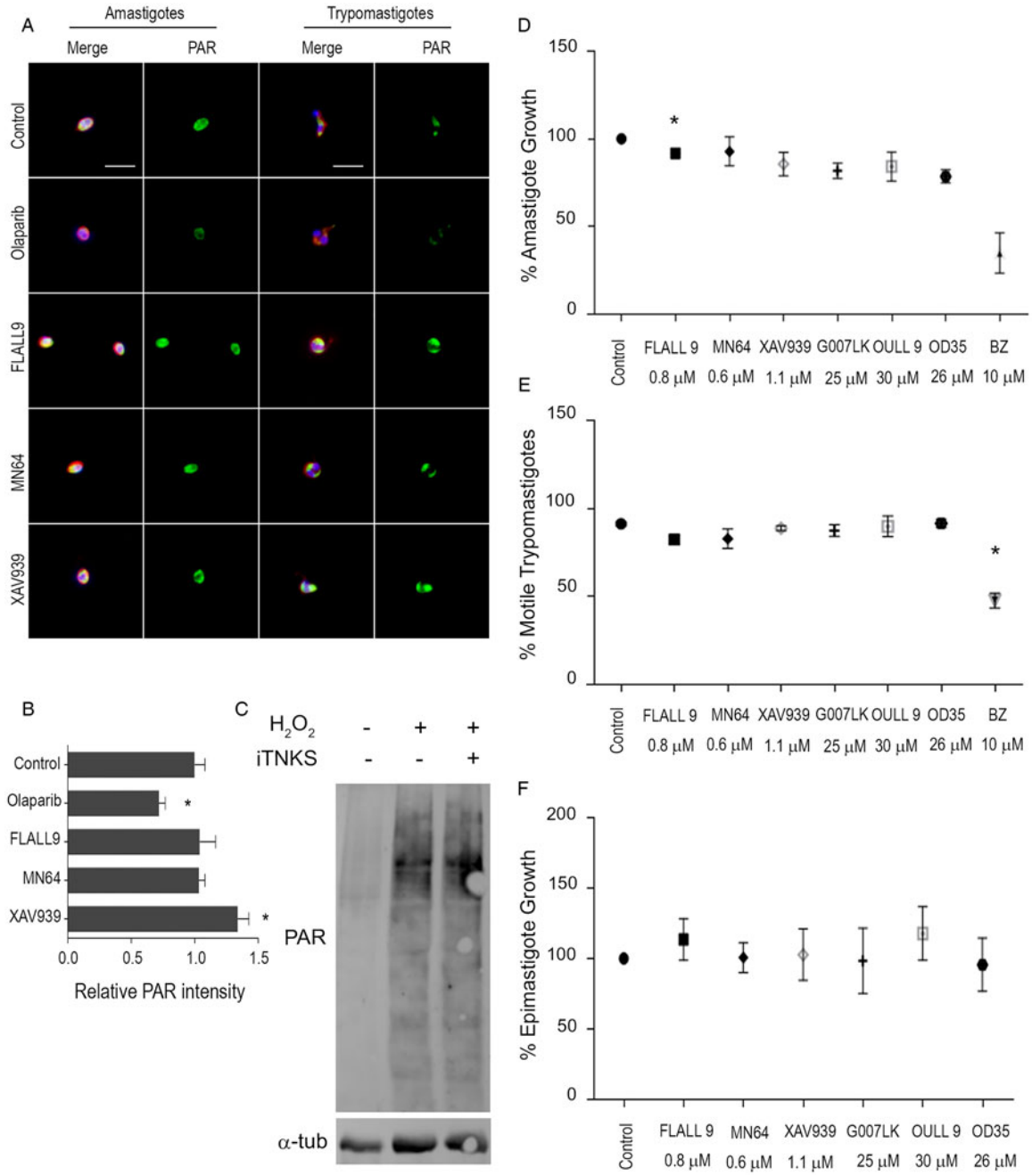

Fig. 2. Effect of TNKSi on TcPARP activity and on the viability of axenic *T. cruzi* cultures. (A) PAR synthesis in amastigote and trypomastigote forms was not diminished by the presence of 0.8 μM FLALL9, 0.6 μM MN64 nor by 1.1 μM XAV939, as evidenced by ICF using an anti-PAR reagent (green). DAPI (blue) was used to stain nuclei and anti-*T. cruzi* serum (red) was used to delineate parasites. Olaparib (0.025 μM), a known PARP-1 and TcPARP inhibitor, reduced PAR formation in both *T. cruzi* forms. Bar: 10 μm. (B) Quantification of PAR intensity in amastigotes treated with a PARP-1 or with TNKS inhibitors, relative to parasites in the absence of inhibitors, using ImageJ software. Mean ± standard error is shown. Data correspond to at least 30 individual parasites per condition. *$P < 0.05$ according to one-way ANOVA and Dunnett statistical tests. (C) TcPARP activity in epimastigotes, evaluated by Western blots with anti-PAR reagent in response to 300 μM H_2O_2 (10 min) was not affected by the presence of 0.6 μM MN64. (D) Extracellular amastigotes (1×10^6 parasites/well) were incubated in a 96-well plate in the presence of TNKSi or benznidazole (BZ) during 48 h and their viability was assessed by Alamar blue. (E) Trypomastigotes (1×10^6 parasites mL^{-1}) obtained from infected cell culture supernatants were incubated in a 96-well plate in the presence of TNKSi or BZ for 5 h, after which motile trypomastigotes were counted in a Neubauer chamber. (F) Exponential growth phase epimastigote cultures (5×10^6 parasites/well) were incubated in a 96-well plate in the presence of TNKSi for 96 h and their viability was assessed by Alamar blue. Results shown in D, E and F are mean ± standard error from three independent experiments, each performed in triplicates and analysed by one-way ANOVA and Dunnett statistical tests. *$P < 0.05$.

reduction of the infection was mainly due to the inhibition of host cell Tankyrases. In contrast with higher eukaryotes, *T. cruzi* bears only one known PARP (TcPARP) (Fernández Villamil *et al.*, 2008). Although a search was conducted on the available *T. cruzi* genomic databases using sequences of full-length human TNKS-1/2 or its catalytic and ankyrin-repeat domains as baits, no positive hits were found. We have previously reported that TcPARP is susceptible to known PARP-1/2 inhibitors but not to the Tankyrase inhibitor IWR-1, and only partially to 1 μM XAV939 (Vilchez Larrea *et al.*, 2012). To corroborate that the compounds here used were not targeting TcPARP, the effect on PAR levels in trypomastigotes and extracellular amastigotes of FLALL 9, MN64 and XAV939, which showed the largest effects against infection, was tested. PAR levels were evaluated by immunofluorescence using a pan-PAR detecting reagent (Gibson *et al.*, 2017) and quantified using ImageJ software. TNKSi FLALL 9 and MN64 did not cause any observable reduction in the amount of PAR present in amastigotes or

https://doi.org/10.1017/S0031182021001402 Published online by Cambridge University Press

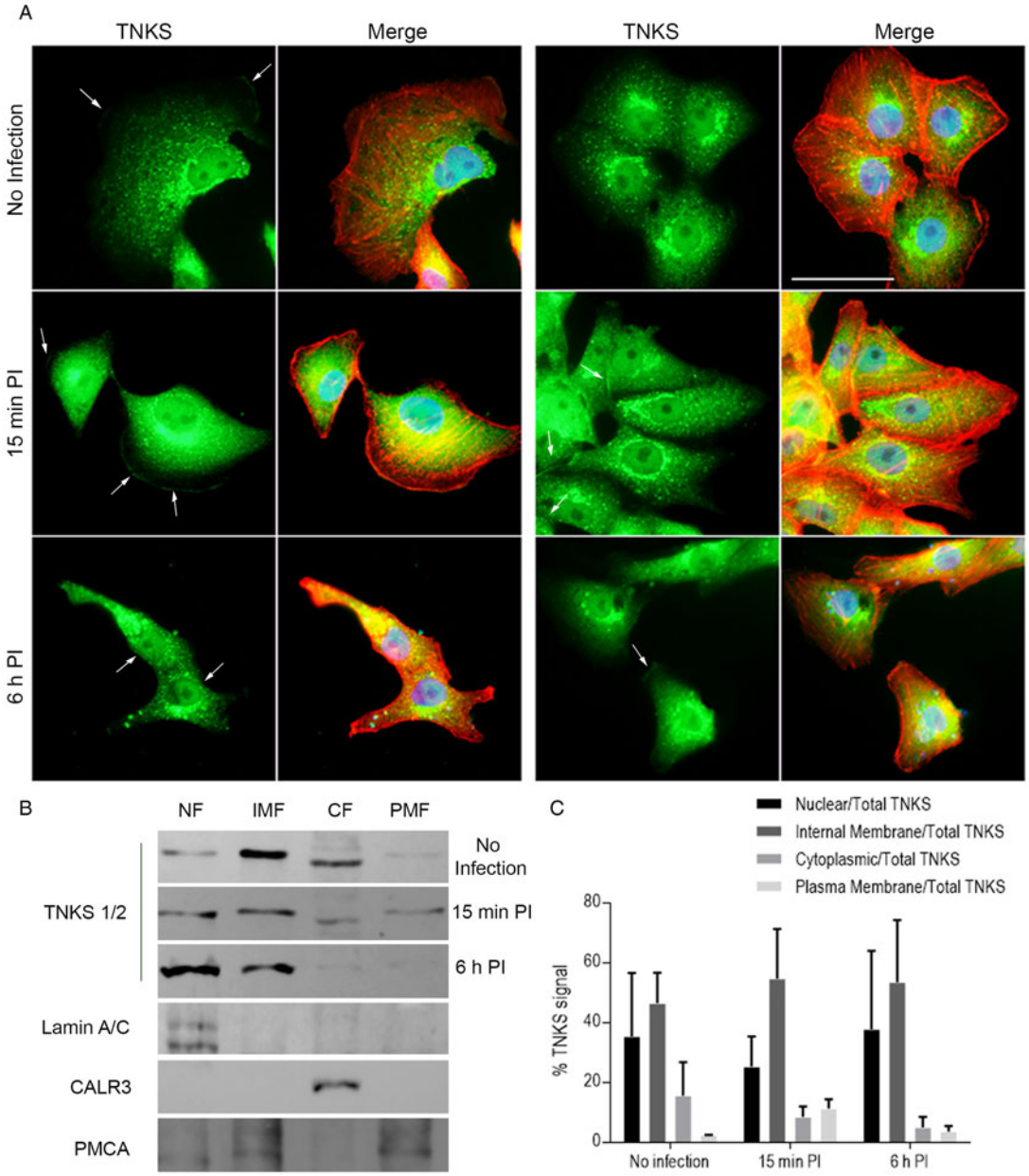

Fig. 3. Vero cell TNKS shifted towards the plasma membrane 15 min post-infection. (A) TNKS localization during initial steps of *T. cruzi* infection (0, 15 min and 6 h p.i.) in Vero cell monolayers was assessed by ICF using an anti-TNKS antibody (green). Nuclei were stained with DAPI (blue) and actin cytoskeleton was detected using Phalloidin (red). White arrows indicate TNKS detected at plasma membrane stretches. Bar: 50 μm. (B) TNKS subcellular localization was evaluated in nuclear (NF), cytoplasmic (CF), internal membrane (IMF) and plasma membrane fractions (PMF) by Western blot using anti-TNKS antibody at 0, 15 min and 6 h post-infection. The fractionation procedure was validated using the correspondent fraction markers, namely lamin A/C, calreticulin A (CALR3) and PMCA, for NF, CF and PMF, respectively. Representative result from two independent experiments. (C) Relative quantification of TNKS signal in the subcellular fractions over total TNKS (calculated as percentage) as evaluated by Western blot. Data from two independent experiments expressed as mean ± S.D.

trypomastigotes, as shown in Fig. 2A and B. In fact, XAV939 appeared to cause an increase in the detected PAR intensity (34% higher than untreated amastigotes). Olaparib, a well-studied PARP-1 inhibitor which we have previously demonstrated to inhibit recombinant TcPARP (Vilchez Larrea *et al.*, 2012), diminished PAR signal associated to amastigotes under the same incubation scheme by 29% when compared to parasites in the absence of any drug or treatment. The synthesis of PAR in epimastigotes in response to a genotoxic stimulus was evaluated by Western blot, in the presence or absence of MN64, one of the TNKSi that displayed the most pronounced infection diminutions. No differences in the intensity of PAR signal were observed between the hydrogen peroxide-stimulated epimastigotes in the presence of 0.6 μM MN64 when compared to epimastigotes in the absence of TNKSi, indicating that overall TcPARP activity was not affected by this TNKSi (Fig. 2C).

Although TNKSi were not inhibiting PAR formation according to our results, the possibility that the TNKSi could still be affecting parasites' viability, therefore affecting Vero cell infection, needed to be considered. Hence, the effect of the compounds above tested was evaluated on different life cycle stages of *T. cruzi* parasites in axenic cultures.

Amastigote viability was not significantly diminished by any of the TNKSi, except for FLALL 9 (Fig. 2D). However, the viability decreased only by 8.2%, below the reduction of the infection levels of Vero cells. Benznidazole (BZ), the most employed drug to treat Chagas disease patients, was used as a control and decreased amastigotes viability by 65%. None of the TNKSi

https://doi.org/10.1017/S0031182021001402 Published online by Cambridge University Press

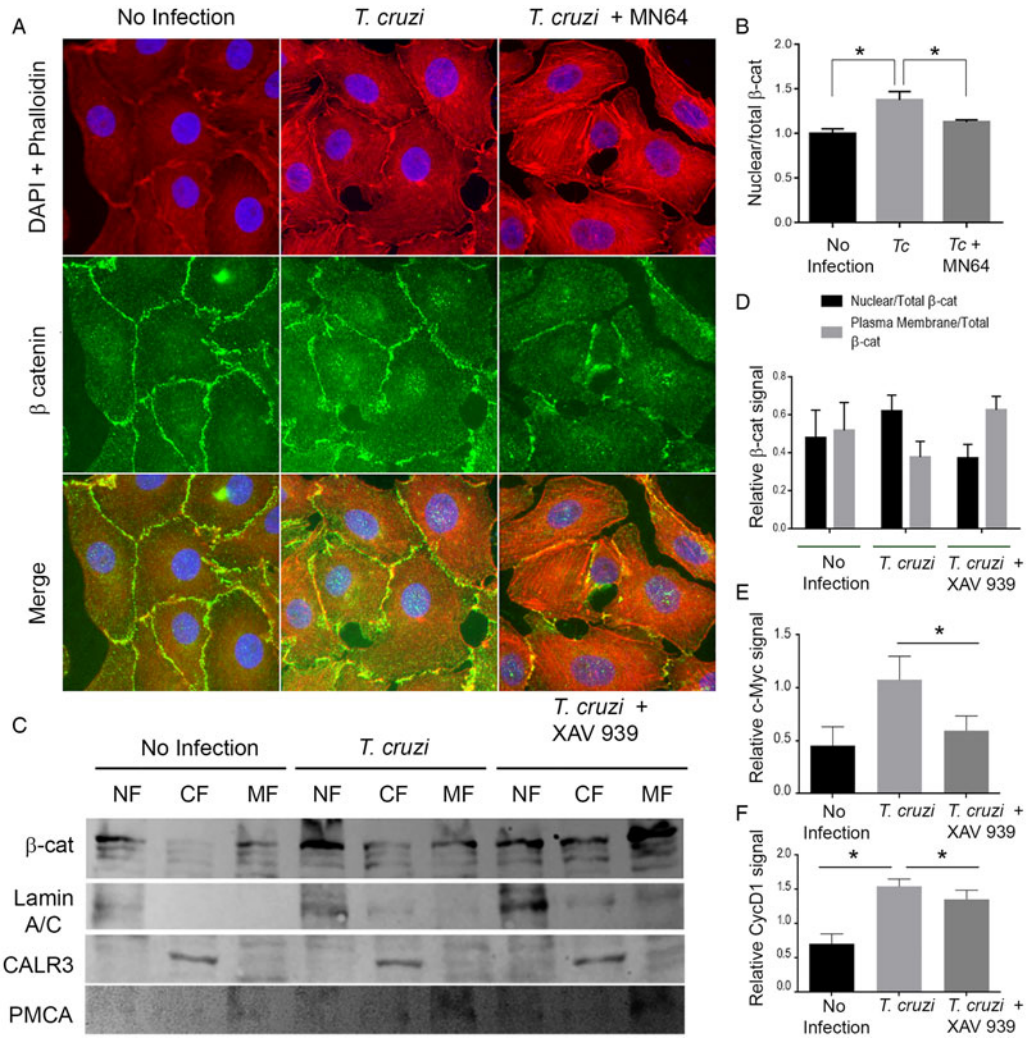

Fig. 4. TNKSi diminished *β*-catenin nuclear translocation that occurred 6 h post-infection in Vero cells in response to *T. cruzi* Tul *β*-gal. (A) *β*-catenin subcellular localization was assessed by ICF, using an anti-*β*-catenin antibody (green), DAPI nuclear counterstain (blue) and phalloidin-546 F-actin probe (red) in (left to right) control Vero cells, *T. cruzi* infected, and infected in the presence of 0.6 μM MN64. (B) Nuclear and total *β*-catenin signal on randomly chosen immunocytofluorescence images was quantified as RawIntDen using ImageJ software. The nuclear/total ratios obtained were normalized to values obtained for samples in the absence of infection or TNKSi. Mean ± standard error is shown. Data are from >100 cells. *$P < 0.05$ according to Student's *t*-test. (C) Western blot against *β*-catenin done on subcellular fraction extracts in control Vero cells, *T. cruzi*-infected (6 h post-infection) and *T. cruzi*-infected cells in the presence of 1.1 μM XAV939. The fractionation procedure was validated using fraction markers: lamin A/C (nuclear fraction; NF), PMCA (membrane fraction; MF) and calreticulin A (cytoplasmic fraction; CF). (D) Relative quantification of nuclear *β*-catenin and membrane-associated *β*-catenin over total *β*-catenin, normalized to the corresponding fraction marker. Data are from three independent experiments. (E) Relative quantification of Western blot band intensity of c-Myc and (F) CyclinD1, normalized to GAPDH, in the presence or absence of infection and/or 1.1 μM XAV939 (total extracts obtained at 24 h p.i). Mean ± standard error is shown. Data shown in E and F are from five independent experiments. *$P < 0.05$, according to one-way ANOVA followed by Fisher's LSD multiple comparison test.

reduced trypomastigote motility either, while BZ diminished the percentage of motile parasites significantly (only 51.6% trypomastigotes retained motility when compared to controls) (Fig. 2E). None of the TNKSi showed toxicity on *T. cruzi* epimastigotes at the concentrations here tested either (Fig. 2F). Altogether, our results suggested that TNKSi were not decreasing infection levels by actioning on the parasites directly but rather by interfering with the functioning of the host cell.

Tankyrase relocated to the vicinity of the host cell membrane during early infection

We have recently reported that TNKS associates to the plasma membrane and is responsible for the formation of a PAR belt associated to the F-actin belt (Vilchez Larrea *et al.*, 2021). To test if this localization changed during *T. cruzi* infection, the subcellular localization of TNKS during the initial steps of this parasite's host cell invasion was assessed by immunocytofluorescence. In the absence of infection, TNKS was detected in several localizations: the strongest signal was observed in a polarized perinuclear location, most likely corresponding to Golgi/ER, but it was also detected as dispersed puncta in the cytoplasm and in the nucleus (Fig. 3A, upper panels). TNKS was also detected associated to short stretches of plasma membrane (white arrows). Shortly after placing the trypomastigotes in contact with the cells, during the cell invasion step (15 min p.i.), a larger number of sections of plasma membrane associated to TNKS could be detected, which also appeared to be longer (Fig. 3A, middle panels). At 6 h post-infection, less plasma membrane-associated TNKS signals were detected, similarly to what was observed in the absence of infection (Fig. 3A, lower panels), suggesting the increase in plasma membrane localization was temporary. Western blot experiments on nuclear, cytoplasmic, internal membrane and plasma membrane fractions of Vero cells, obtained at 0, 15 min and 6 h p.i. supported the results obtained by ICF (Fig. 3B and C). Under control conditions (no infection), TNKS was mainly associated to the internal membrane and nuclear fractions. At 15 min p.i., TNKS signal associated to the plasma membrane

https://doi.org/10.1017/S0031182021001402 Published online by Cambridge University Press

fraction increased (from 2.4% in the absence of infection to 11.4% at 15 min p.i.), while the association to nuclear fraction diminished. After trypomastigote internalization (6 h p.i.), association to this fraction decreased (3.8%) while the association to the nuclear fraction increased (Fig. 3C). These results indicated that TNKS could be responding to *T. cruzi* cell invasion by changing its localization to the cell membrane, where it could exert particular functions.

β-catenin nuclear translocation in response to T. cruzi infection was reduced in the presence of TNKSi

Wnt/β-catenin signalling acts as a modulator of the inflammatory response triggered by *T. cruzi* infection in bone marrow-derived macrophages and supports intracellular parasite replication (Volpini *et al.*, 2018). Since TNKS is associated to the positive regulation of canonical Wnt signalling in other cellular models (Yang *et al.*, 2016; Mariotti *et al.*, 2017), β-catenin subcellular localization at 0 and 6 h p.i. was evaluated in the absence or presence of TNKSi by indirect immunocytofluorescence (Fig. 4A and B) and Western blot after subcellular fractionation (Fig. 4C and D).

Quantification of the nuclear/total β-catenin signal on ICF evidenced β-catenin nuclear accumulation in Vero cells 6 h post-infection (Fig. 4B). The TNKSi MN64 hampered the observed β-catenin translocation, diminishing β-catenin nuclear accumulation significantly.

β-catenin nuclear re-localization in Vero cells in response to *T. cruzi* infection was confirmed by Western blot on nuclear, cytoplasmic and cell membrane fractions (Fig. 4C). Relative quantification against the different subcellular fraction markers (Fig. 4D) showed that, while β-catenin association to the plasma membrane fraction appeared to decrease, its association to the nuclear fraction increased at 6 h p.i., supporting what was observed by ICF. This re-localization was consistently hindered by the presence of 1.1 μM XAV939 across experiments, as nuclear β-catenin decreased, and membrane-associated β-catenin augmented. Although the results obtained by Western blot were not statistically significant, mainly due to variations in untreated, uninfected cultures, TNKSi diminished relative nuclear β-catenin signal during *T. cruzi* infection in all experiments performed.

Activation of β-catenin signalling and its translocation to the nucleus leads to the upregulation of target genes, such as c-Myc and CyclinD1 (MacDonald *et al.*, 2009). Therefore, the nuclear accumulation of this protein observed during *T. cruzi* infection was expected to be accompanied by the increased expression of these proteins (Fig. 4E and F). Relative quantification of c-Myc on total Vero cell extracts obtained at 24 h p.i. showed that its expression was higher in infected cells than in uninfected cell cultures (2.38-fold increase). The presence of XAV939 reduced the expression of this protein significantly in infected cultures by 48% (Fig. 4E). Expression of CyclinD1 was also upregulated in our infection model (2.18-fold) and slightly decreased when infection occurred in the presence of XAV939 (12.26% reduction). These results show that TNKSi are effectively reducing β-catenin signalling during *T. cruzi* infection in Vero cells.

These results indicated that, similar to what occurs in macrophages (Volpini *et al.*, 2018), β-catenin nuclear concentration and its transcriptional activity in non-professional phagocytic cells increased in response to *T. cruzi* infection and that the inhibition of TNKS affected this behaviour negatively.

TNF-α increased during T. cruzi infection and was partially modulated by TNKSi

Since it was demonstrated that β-catenin signalling upregulated TNF-α expression during *T. cruzi* infection in BMM (Volpini *et al.*, 2018), the expression of this cytokine was tested by RT-qPCR in our model as a proof of concept. Cells were collected at 24 h post-infection, following the schedule in Volpini *et al.* (2018), in the presence or absence of MN64. TNF-α mRNA levels in Vero cells increased significantly during *T. cruzi* infection and 0.6 μM MN64 led to a significant reduction in TNF-α mRNA levels, even below the ones detected in the absence of *T. cruzi* infection (Fig. 5A).

To corroborate the results obtained by RT-qPCR, the amount of TNF-α present in the cell culture supernatant was also quantified by capture ELISA on samples obtained at 24 h p.i., in the presence or absence of XAV939, another TNKSi that demonstrated efficacy against *in vitro* infection in Vero cells. *Trypanosoma cruzi* infection caused a mild but significant increase in the amount of TNF-α detected in the cell culture supernatant when compared to cultures in the absence of infection (3.46 *vs* 3.29 pg mL^{-1}, respectively, $p = 0.0033$). The presence of the TNKSi XAV939 during *T. cruzi* infection reduced the amount of TNF-α in the culture to levels similar to the ones observed in the absence of infection (3.30 pg mL^{-1}) (Fig. 5B). These results confirmed that TNKSi can hamper TNF-α expression during *T. cruzi* infection.

Because TNF-α role in the modulation of *T. cruzi* infection depends strongly – among other factors – on the host cell involved, we needed to confirm if this cytokine could modulate the infection levels in Vero cells. Exogenous addition of 20 ng mL^{-1} TNF-α markedly enhanced *T. cruzi* infection (Fig. S3). These results indicated that TNF-α facilitated *T. cruzi* infection in Vero cells at least *in vitro*, in agreement with what has been published for HEK293 T and LLC-MK2 cells (Pinto *et al.*, 2011). Therefore, as TNKSi reduced the expression and secretion of the pro-infection cytokine TNF-α in our model, this could be, in turn, reducing *T. cruzi* infection of Vero cells. These results could be hinting at one of the mechanisms that explains the ability of TNKSi to hinder *T. cruzi* infection in our model.

Discussion

In the present work, it was shown for the first time that inhibition of host cell Tankyrase hampered *T. cruzi* infection *in vitro* as well as nuclear accumulation of β-catenin and TNF-α expression, two signals associated to successful infections. Five out of six TNKSi here tested led to a significant decrease in the infection, with MN64 and FLALL 9 being the TNKSi that exerted the largest effect without affecting Vero cell viability at 100 × IC_{50} concentrations. A significant decrease in the number of cell-associated parasites was also observed when cells were incubated with MN64 only before initiating *T. cruzi* infection. However, parasite viability was not affected in a direct manner by most of the TNKSi here tested. Altogether, these results support that TNKSi-induced downregulation of the infection occurred through the modulation of host cell PAR metabolism and related signalling pathways.

Activation of Wnt/β-catenin pathway downregulates the activity of the β-catenin destruction complex. Upon Wnt activation, Axin is recruited to a plasma membrane signalosome complex and β-catenin is no longer targeted for degradation, enabling its accumulation in the nucleus (MacDonald *et al.*, 2009). Nuclear β-catenin associates to TCF/Lef1 (T-cell factor/lymphoid enhanced factor1) and upregulates the expression of numerous genes (MacDonald *et al.*, 2009). TNKS acts as a positive regulator of canonical Wnt signalling by destabilizing the β-catenin destruction complex mainly through the PARylation of Axin (Yang *et al.*, 2016; Mariotti *et al.*, 2017) or adenomatous polyposis coli (Croy *et al.*, 2016). Recent findings in a *T. cruzi* bone marrow-derived macrophage (BMM) infection model show that β-catenin accumulates in the nucleus at 2–12 h post-infection

https://doi.org/10.1017/S0031182021001402 Published online by Cambridge University Press

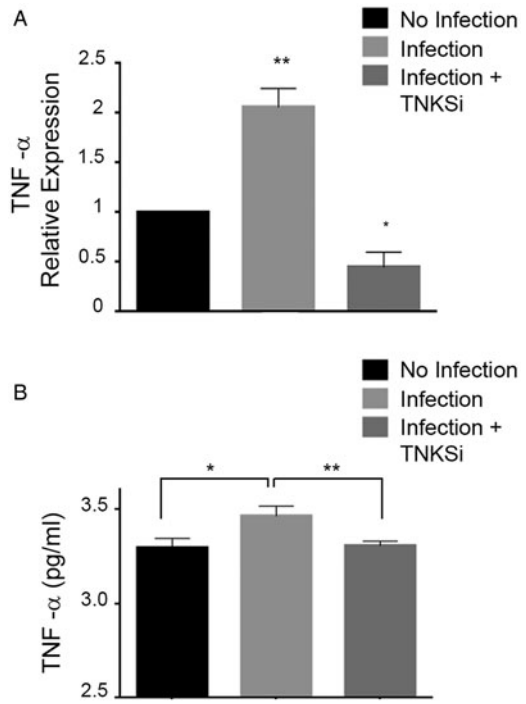

Fig. 5. *Trypanosoma cruzi* Tul β-gal infection induced expression of TNF-α, which decreased in the presence of TNKSi. (A) TNF-α mRNA level was evaluated by qPCR at 24 h p.i. in the presence or absence of 0.6 μM MN64. Cytokine expression was normalized against GAPDH expression. Mean ± standard error is shown. Data are from three independent experiments in duplicate (B) TNF-α presence in the cell culture supernatant were evaluated by a colourimetric capture ELISA at 24 h p.i. in the presence or absence of 1.1 μM XAV939. Sample absorbances (450 nm) were compared to a recombinant TNF-α curve. Mean ± standard error is shown. Data are from three independent experiments performed in triplicates. *$P < 0.05$; **$P < 0.01$, according to one-way ANOVA followed by Fisher's LSD multiple comparison test. Comparisons were done against the control in the absence of infection.

and enhances the expression of classical targets of this pathway (*Wisp1*, *Axin1*, *Ccnd1*). Disturbing Wnt secretion through porcupine (PORCN) inhibition or β-catenin transcriptional activity inhibition in these macrophages diminishes the parasitic infection (Volpini *et al.*, 2018). In agreement with this report, β-catenin translocated to the nucleus at 6 h post-infection in our epithelial cell infection model. TNKSi counteracted this nuclear accumulation as well as the upregulation of genes known to be under transcriptional control of β-catenin (c-Myc and CyclinD1). Although the mechanisms through which TNKS regulates β-catenin nuclear accumulation during infection still need to be addressed, results reported for BMM (Volpini *et al.*, 2018) together with our findings suggest that TNKS could be targeted to disrupt Wnt/β-catenin signalling during *T. cruzi* infection. However, a crosstalk with other pathways modulating β-catenin translocation such as those activated by growth factors (Zhang *et al.*, 2013) cannot be discarded and should be further explored.

Volpini *et al.* associated the reduction in *T. cruzi* infection of BMM caused by Wnt/β-catenin signalling inhibitors with a decrease in the replication rate of intracellular amastigotes (Volpini *et al.*, 2018). Although TNKSi exerted the largest detrimental effect on Vero cell infection when incubated during the whole infection cycle, a significant decrease in the number of cell-associated parasites was also registered at 1 h p.i. in the presence of MN64. This early effect might be indicating that Tankyrases are participating in early infection-triggered mechanisms during adhesion, signalling or invasion. In heart endothelial cells, YAP (Yes-associated protein) nuclear levels are altered during the early phase of *T. cruzi* Infection (Arun *et al.*, 2020). In immortalized human Schwann cells, *T. cruzi* infection induces a robust activation of Akt (Chuenkova and PereiraPerrin, 2009). Both YAP and Akt can be modulated by TNKSi (Kim, 2018). It is therefore possible that TNKSi are also regulating YAP and Akt pathways in *T. cruzi*-infected Vero cells.

The observed reduction of *T. cruzi* infection caused by TNKSi could not be attributed to effects exerted on the parasite itself, as the drugs here tested were not cytotoxic to any of the parasite developmental forms. *Trypanosoma cruzi* bears a single classical PARP gene (TcPARP), structurally similar to hPARP-2, which was shown to be involved in the response to DNA damage and the regulation of the cell cycle (Fernández Villamil *et al.*, 2008; Vilchez Larrea *et al.*, 2011). Hybrid or 'TNKS-like' PARP genes have been described in certain species (Citarelli *et al.*, 2010; Perina *et al.*, 2014). An exhaustive search conducted on curated trypanosomes genomic databases (Berná *et al.*, 2018) excluded the existence of TNKS or TNKS-like genes in trypanosomes. Although classical PARP-1 inhibitors affect TcPARP activity both *in vitro* and *in vivo*, TNKSi could not inhibit PAR formation in the different developmental stages of *T. cruzi*, indicating that the parasite's PARP was not affected by the TNKSi here used. This is in agreement with previous observations in which the TNKSi IWR-2 only marginally reduces TcPARP activity at 10 μM while XAV393 only partially inhibits TcPARP at 1 μM *in vitro* (Vilchez Larrea *et al.*, 2012).

The role of pro-inflammatory cytokines in *T. cruzi* infection depends on the host cell: while in macrophages and cardiomyocytes, cytokines such as TNF-α and INF-γ enhance anti-trypanocidal activity and reduce overall infection (Fichera *et al.*, 2004; Volpini *et al.*, 2018), in astrocytes and epithelial cells (HEK293 T and LLC-MK2), these cytokines enhance *T. cruzi* infection, effect that could be counteracted by an anti-TNF antibody (Pinto *et al.*, 2011; Silva *et al.*, 2015). In our Vero cell model, TNF-α exogenous addition increased *T. cruzi* infection (Fig. S3). Our results showed that *T. cruzi* induced TNF-α upregulation in Vero cells in an infection-promoting event. TNKS inhibition hampered the production of this cytokine and, in turn, negatively affected infection. The observed downregulation of TNF-α could partially account for the modulation of *T. cruzi* infection exerted by TNKSi.

TNKS was associated to various localizations in the host cell in basal conditions but appeared to shift towards the plasma membrane fraction during early *T. cruzi* infection (15 min). Recently, we described the existence of a PAR belt associated to the epithelial *adherens junctions* belt and subcortical actin in Vero cells (Lafon-Hughes *et al.*, 2014), observation that was followed by the description of peripheral PAR localization in Schwann cells and oocytes (Lafon Hughes *et al.*, 2017; Xie *et al.*, 2018). Initial results pointed at TNKS as the possible PAR belt-synthesizing enzyme. Our recent report on the association of TNKS to the plasma membrane as well as the TNKS-mediated PARylation of vinculin supports those results (Vilchez Larrea *et al.*, 2021). Both in Vero and in Schwann cells, PAR alterations are associated to actin cytoskeleton remodelling (Lafon-Hughes *et al.*, 2014; Lafon Hughes *et al.*, 2017). Although the role of actin depolymerization during *T. cruzi* infection still remains controversial (Tardieux *et al.*, 1994; Fonseca Rosestolato *et al.*, 2002), TNKS recruitment to the plasma membrane during cell invasion by the parasite could be related to subcortical actin cytoskeleton remodelling during *T. cruzi* infection.

Although inhibitors with different potencies against TNKS-1 and TNKS-2 were employed, our results cannot discern the importance of each one during *T. cruzi* infection. A genetic approach, e.g. knockout by CRISPR/Cas9 or iRNA knockdown, could help to tackle this question. Both enzymes are remarkably similar, with 85% overall identity (Kaminker *et al.*, 2001), and it is yet unclear which of them is participating in the regulation of

https://doi.org/10.1017/S0031182021001402 Published online by Cambridge University Press

the Wnt/β-catenin signalling, although reported data suggest that both, TNKS-1 and TNKS-2, are playing redundant functions in the destabilization of the β-catenin destruction complex (Martino-Echarri *et al.*, 2016).

Evidence that Wnt/β-catenin signalling participates in the modulation of inflammation and infection-related processes is growing. For example, in epithelial cells, β-catenin can induce the secretion of pro-inflammatory cytokines (Moparthi and Koch, 2019). Although *T. cruzi* infection induced TNF-α expression in our model and that this was downregulated by TNKSi, our results do not allow us to ascertain the connection between canonical Wnt signalling and the expression of this cytokine in this model. Evaluating the response to *T. cruzi* infection and TNKS inhibition of other inflammatory mediators and other β-catenin transcriptional targets could help clarify the relationship between the observed phenomena. Other mechanisms through which TNKS regulates *T. cruzi* infection also deserve further study.

The search for new drugs against Chagas' disease has been mainly focused on the exploration of potential therapeutic targets in the parasite itself (Beaulieu *et al.*, 2010; Le Loup *et al.*, 2011). However, given that the establishment of a successful infection relies on the triggering of a concerted network of signalling pathways inside the host cell, modulating these pathways can also become a valuable alternative in the quest for new effective treatments. Our results fit with recent evidence indicating that the interruption of Wnt/β-catenin signalling at different levels in the pathway can protect cell types from *T. cruzi* infection, at least *in vitro* (Volpini *et al.*, 2018).

Aiming at the development of new treatments against various types of tumours, several inhibitors targeting different steps in the Wnt/β-catenin pathway have entered clinical phase trials recently, with mixed results (Jung and Park, 2020).

A Tankyrase inhibitor, E7449, has entered into clinical trials with promising initial results regarding safety and tolerability (Plummer *et al.*, 2020). Therefore, efforts to understand the importance of TNKS and Wnt/β-catenin during *T. cruzi* infection can contribute to a drug repurposing strategy, shortening the time and diminishing the economic burden associated to *de novo* development of anti-parasitic drugs.

This work disclosed for the first time the anti-*T. cruzi* infection effects of TNKSi. Although several mechanisms may be involved, our results evidenced that TNKSi counteracted infection-induced signals: increase of nuclear-translocated β-catenin and expression of the cytokine TNF-α in Vero epithelial cells. We have previously reported that host PARP-1 and PARG inhibition or silencing diminished *T. cruzi* infection in epithelial cells (Vilchez Larrea *et al.*, 2013, 2012). The results presented here indicate that host Tankyrases, also members of the PARP family, are engaged during *T. cruzi* infection too, adding evidence to support PAR metabolism as a piece of the signalling puzzle elicited in the host during this parasitic infection. Moreover, the promising entrance of TNKSi in clinical assays against tumours encourages further research that could eventually lead to TNKSi repurposing as anti-chagasic drugs.

Supplementary material. The supplementary material for this article can be found at https://doi.org/10.1017/S0031182021001402.

Data. The authors confirm that all relevant data are included in the article and/or its supplementary information files.

Acknowledgements. The authors are grateful to Dr Lari Lehtiö for providing Tankyrase inhibitors and to Dr Carlos Robello for performing the detailed search for Tankyrases in the *Trypanosoma cruzi* genome database. We would also like to thank Dr Guillermo Alonso for carefully revising the manuscript.

Author contribution. L.L.H. and S.C.V.L. conceived, designed the study and conducted data gathering. L.L.H., S.H.F.V. and S.C.V.L. performed statistical analyses and wrote the article.

Financial support. This work was supported by Consejo Nacional de Investigaciones Científicas y Técnicas (CONICET), Argentina (Grant PCB-I. 2017-2019-SVL) and Agencia Nacional de Investigación e Innovación (ANII) Grant (|MOV_CO_2015_1_110430. 2017-2019 – LLH).

Conflict of interest. None.

Ethical standards. Not applicable.

References

Arun A, Rayford KJ, Cooley A, Rachakonda G, Villalta F, Pratap S, Lima MF, Sheibani N and Nde PN (2020) Thrombospondin-1 plays an essential role in yes-associated protein nuclear translocation during the early phase of *Trypanosoma cruzi* infection in heart endothelial cells. *International Journal of Molecular Sciences* **21**, 1–15.

Beaulieu C, Isabel E, Fortier A, Massé F, Mellon C, Méthot N, Ndao M, Nicoll-Griffith D, Lee D, Park H and Black WC (2010) Identification of potent and reversible cruzipain inhibitors for the treatment of Chagas disease. *Bioorganic & Medicinal Chemistry Letters* **20**, 7444–7449.

Berná L, Rodriguez M, Chiribao ML, Parodi-Talice A, Pita S, Rijo G, Alvarez-Valin F and Robello C (2018) Expanding an expanded genome: long-read sequencing of *Trypanosoma cruzi*. *Microbial Genomics* **4**, 1–19. doi: https://doi.org/10.1099/mgen.0.000177

Brady PN, Goel A and Johnson MA (2018) Poly(ADP-ribose) polymerases in host-pathogen interactions, inflammation, and immunity. *Microbiology and Molecular Biology Reviews* **83**, 1–48.

Buckner FS, Verlinde CL, La Flamme AC and Van Voorhis WC (1996) Efficient technique for screening drugs for activity against *Trypanosoma cruzi* using parasites expressing b-galactosidase. *Microbiology* **40**, 2592–2597.

Burleigh BA and Woolsey AM (2002) Cell signalling and *Trypanosoma cruzi* invasion. *Cellular Microbiology* **4**, 701–711.

Chuenkova MV and PereiraPerrin M (2009) *Trypanosoma cruzi* targets Akt in host cells as an intracellular antiapoptotic strategy. *Science Signaling* **2**, ra74.

Citarelli M, Teotia S and Lamb RS (2010) Evolutionary history of the poly (ADP-ribose) polymerase gene family in eukaryotes. *BMC Evolutionary Biology* **10**, 308.

Croy HE, Fuller CN, Giannotti J, Robinson P, Foley AVA, Yamulla RJ, Cosgriff S, Greaves BD, Von Kleeck RA, An HH, Powers CM, Tran JK, Tocker AM, Jacob KD, Davis BK and Roberts DM (2016) The poly (ADP-ribose) polymerase enzyme Tankyrase antagonizes activity of the β-catenin destruction complex through ADP-ribosylation of Axin and APC2. *Journal of Biological Chemistry* **291**, 12747–12760.

De Boeck G, Forsyth RG, Praet M and Hogendoorn PCW (2009) Telomere-associated proteins: cross-talk between telomere maintenance and telomere-lengthening mechanisms. *The Journal of Pathology* **217**, 327–344.

de Souza W, de Carvalho TMU and Barrias ES (2010) Review on *Trypanosoma cruzi*: host cell interaction. *International Journal of Cell Biology* **2010**, 1–18. doi: https://doi.org/10.1155/2010/295394

Fernández Villamil SH, Baltanás R, Alonso GD, Vilchez Larrea SC, Torres HN and Flawiá MM (2008) TcPARP: a DNA damage-dependent poly (ADP-ribose) polymerase from *Trypanosoma cruzi*. *International Journal for Parasitology* **38**, 277–287.

Fichera LE, Albareda MC, Laucella SA and Postan M (2004) Intracellular growth of *Trypanosoma cruzi* in cardiac myocytes is inhibited by cytokine-induced nitric oxide release. *Infection and Immunity* **72**, 359–363.

Fonseca Rosestolato CT, Da Matta Furniel Dutra J, De Souza W and Ulisses De Carvalho TM (2002) Participation of host cell actin filaments during interaction of trypomastigote forms of *Trypanosoma cruzi* with host cells. *Cell Structure and Function* **27**, 91–98.

Gibson BA, Conrad LB, Huang D and Kraus WL (2017) Generation and characterization of recombinant antibody-like ADP-ribose binding proteins. *Biochemistry* **56**, 6305–6316.

Haikarainen T, Koivunen J, Narwal M, Venkannagari H, Obaji E, Joensuu P, Pihlajaniemi T and Lehtiö L (2013) Para-substituted 2-phenyl-3,4-dihydroquinazolin-4-ones as potent and selective tankyrase inhibitors. *ChemMedChem* **8**, 1978–1985.

Haikarainen T, Krauss S and Lehtio L (2014) Tankyrases: structure, function and therapeutic implications in cancer. *Current Pharmaceutical Design* **20**, 6472–6488.

Haikarainen T, Waaler J, Ignatev A, Nkizinkiko Y, Venkannagari H, Obaji E, Krauss S and Lehtiö L (2016) Development and structural analysis of

adenosine site binding tankyrase inhibitors. *Bioorganic & Medicinal Chemistry Letters* **26**, 328–333.

Hsiao SJ and Smith S (2008) Tankyrase function at telomeres, spindle poles, and beyond. *Biochimie* **90**, 83–92.

Jansen AM, Xavier SCDC and Roque ALR (2018) *Trypanosoma cruzi* transmission in the wild and its most important reservoir hosts in Brazil. *Parasites and Vectors* **11**, 1–25.

Jung YS and Park JIL (2020) Wnt signaling in cancer: therapeutic targeting of Wnt signaling beyond β-catenin and the destruction complex. *Experimental & Molecular Medicine* **52**, 183–191.

Kaminker PG, Kim SH, Taylor RD, Zebarjadian Y, Funk WD, Morin GB, Yaswen P and Campisi J (2001) TANK2, a New TRF1-associated poly (ADP-ribose) polymerase, causes rapid induction of cell death upon overexpression. *Journal of Biological Chemistry* **276**, 35891–35899.

Kim MK (2018) Novel insight into the function of Tankyrase (review). *Oncology Letters* **16**, 6895–6902.

Lafon-Hughes L, Vilchez Larrea SC, Kun A and Fernández Villamil SH (2014) VERO cells harbor a poly-ADP-ribose belt partnering their epithelial adhesion belt. *PeerJ* **2**, e617.

Lafon Hughes LI, Romeo Cardeillac CJ, Cal Castillo KB, Vilchez Larrea SC, Sotelo Sosa JR, Folle Ungo GA, Fernández Villamil SH and Kun González AE (2017) Poly(ADP-ribosylation) is present in murine sciatic nerve fibers and is altered in a Charcot-Marie-Tooth-1E neurodegenerative model. *PeerJ* **5**, e3318.

Lehtiö L, Chi NW and Krauss S (2013) Tankyrases as drug targets. *FEBS Journal* **280**, 3576–3593.

Le Loup G, Pialoux G and Lescure FX (2011) Update in treatment of Chagas disease. *Current Opinion in Infectious Diseases* **24**, 428–434.

Levaot N, Voytyuk O, Dimitriou I, Sircoulomb F, Chandrakumar A, Deckert M, Krzyzanowski PM, Scotter A, Gu S, Janmohamed S, Cong F, Simoncic PD, Ueki Y, La Rose J and Rottapel R (2011) Loss of Tankyrase-mediated destruction of 3BP2 is the underlying pathogenic mechanism of cherubism. *Cell* **147**, 1324–1339.

Li Z, Yamauchi Y, Kamakura M, Murayama T, Goshima F, Kimura H and Nishiyama Y (2012) Herpes simplex virus requires poly(ADP-ribose) polymerase activity for efficient replication and induces extracellular signal-related kinase-dependent phosphorylation and ICP0-dependent nuclear localization of Tankyrase 1. *Journal of Virology* **86**, 492–503.

Lüscher B, Bütepage M, Eckei L, Krieg S, Verheugd P and Shilton BH (2018) ADP-ribosylation, a multifaceted posttranslational modification involved in the control of cell physiology in health and disease. *Chemical Reviews* **118**, 1092–1136.

Ma B and Hottiger MO (2016) Crosstalk between wnt/β-catenin and NF-κB signaling pathway during inflammation. *Frontiers in Immunology* **7**, 1–14. doi: https://doi.org/10.3389/fimmu.2016.00378

MacDonald BT, Tamai K and He X (2009) Wnt/β-catenin signaling: components, mechanisms, and diseases. *Developmental Cell* **17**, 9–26.

Mariotti L, Pollock K and Guettler S (2017) Regulation of Wnt/β-catenin signalling by tankyrase-dependent poly(ADP-ribosyl)ation and scaffolding. *British Journal of Pharmacology* **174**, 4611–4636.

Martino-Echarri E, Brocardo MG, Mills KM and Henderson BR (2016) Tankyrase inhibitors stimulate the ability of Tankyrases to bind Axin and drive assembly of β-catenin degradation-competent Axin Puncta. *PLoS ONE* **11**, e0150484.

Miettinen M, Vedantham M and Pulliainen AT (2019) Host poly (ADP-ribose) polymerases (PARPs) in acute and chronic bacterial infections. *Microbes and Infection* **21**(10), 423–431. https://doi.org/10.1016/j.micinf.2019.06.002

Moparthi L and Koch S (2019) Wnt signaling in intestinal inflammation. *Differentiation* **108**, 24–32.

Nkizinkiko Y, Suneel Kumar BVS, Jeankumar VU, Haikarainen T, Koivunen J, Madhuri C, Yogeeswari P, Venkannagari H, Obaji E, Pihlajaniemi T, Sriram D and Lehtiö L (2015) Discovery of potent and selective nonplanar tankyrase inhibiting nicotinamide mimics. *Bioorganic & Medicinal Chemistry* **23**, 4139–4149.

Palazzo L, Mikoč A and Ahel I (2017) ADP-ribosylation: new facets of an ancient modification. *FEBS Journal* **284**, 2932–2946.

Perina D, Mikoč A, Ahel J, Ćetković H, Žaja R and Ahel I (2014) Distribution of protein poly(ADP-ribosyl)ation systems across all domains of life. *DNA Repair* **23**, 4–16.

Pinto AMT, Sales PCM, Camargos ERS and Silva AM (2011) Tumour necrosis factor (TNF)-mediated NF-κB activation facilitates cellular invasion of non-professional phagocytic epithelial cell lines by *Trypanosoma cruzi*. *Cellular Microbiology* **13**, 1518–1529.

Plummer R, Dua D, Cresti N, Drew Y, Stephens P, Foegh M, Knudsen S, Sachdev P, Mistry BM, Dixit V, McGonigle S, Hall N, Matijevic M, McGrath S and Sarker D (2020) First-in-human study of the PARP/tankyrase inhibitor E7449 in patients with advanced solid tumours and evaluation of a novel drug-response predictor. *British Journal of Cancer* **123**, 525–533.

Riffell JL, Lord CJ and Ashworth A (2012) Tankyrase-targeted therapeutics: expanding opportunities in the PARP family. *Nature Reviews Drug Discovery* **11**, 923–936.

Romano PS, Cueto JA, Casassa AF, Vanrell MC, Gottlieb RA and Colombo MI (2012) Molecular and cellular mechanisms involved in the *Trypanosoma cruzi*/host cell interplay. *IUBMB Life* **64**, 387–396.

Roy S, Liu F and Arav-Boger R (2015) Human cytomegalovirus inhibits the PARsylation activity of tankyrase – a potential strategy for suppression of the wnt pathway. *Viruses* **8**, 1–17. doi: https://doi.org/10.3390/v8010008

Santi-Rocca J, Fernandez-Cortes F, Chillón-Marinas C, González-Rubio M-L, Martin D, Gironès N and Fresno M (2017) A multi-parametric analysis of *Trypanosoma cruzi* infection: common pathophysiologic patterns beyond extreme heterogeneity of host responses. *Scientific Reports* **7**, 8893.

Sbodio JI, Lodish HF and Chi N (2002) Tankyrase-2 oligomerizes with tankyrase-1 and binds to both TRF1 (telomere-repeat-binding factor 1) and IRAP (insulin-responsive aminopeptidase). *Biochemical Journal* **361**, 451–459.

Silva RR, Mariante RM, Silva AA, dos Santos ALB, Roffê E, Santiago H, Gazzinelli RT and Lannes-Vieira J (2015) Interferon-gamma promotes infection of astrocytes by *Trypanosoma cruzi*. *PLoS ONE* **10**, e0118600.

Takagi Y, Akutsu Y, Doi M and Furukawa K (2019) Utilization of proliferable extracellular amastigotes for transient gene expression, drug sensitivity assay, and CRISPR/Cas9-mediated gene knockout in *Trypanosoma cruzi*. *PLoS Neglected Tropical Diseases* **13**, 1–21.

Tardieux I, Nathanson MH and Andrews NW (1994) Role in host cell invasion of *Trypanosoma cruzi*-induced cytosolic-free Ca2+transients. *Journal of Experimental Medicine* **179**, 1017–1022.

Thorsell A-G, Ekblad T, Karlberg T, Löw M, Pinto AF, Trésaugues L, Moche M, Cohen MS and Schüler H (2017) Structural basis for potency and promiscuity in poly(ADP-ribose) polymerase (PARP) and Tankyrase inhibitors. *Journal of Medicinal Chemistry* **60**, 1262–1271.

Vilchez Larrea SC, Alonso GD, Schlesinger M, Torres HN, Flawiá MM and Fernández Villamil SH (2011) Poly(ADP-ribose) polymerase plays a differential role in DNA damage-response and cell death pathways in *Trypanosoma cruzi*. *International Journal for Parasitology* **41**, 405–416.

Vilchez Larrea SC, Haikarainen T, Narwal M, Schlesinger M, Venkannagari H, Flawiá MM, Villamil SHF and Lehtiö L (2012) Inhibition of poly (ADP-ribose) polymerase interferes with *Trypanosoma cruzi* infection and proliferation of the parasite. *PLoS ONE* **7**, e46063.

Vilchez Larrea SC, Schlesinger M, Kevorkian ML, Flawiá MM, Alonso GD and Fernández Villamil SH (2013) Host cell poly(ADP-ribose) glycohydrolase is crucial for *Trypanosoma cruzi* infection cycle. *PLoS ONE* **8**, e67356.

Vilchez Larrea S, Valsecchi WM, Fernández Villamil SH and Lafon Hughes LI (2021) First body of evidence suggesting a role of a tankyrase-binding motif (TBM) of vinculin (VCL) in epithelial cells. *PeerJ* **9**, e11442.

Volpini X, Ambrosio LF, Fozzatti L, Insfran C, Stempin CC, Cervi L and Motran CC (2018) *Trypanosoma cruzi* exploits Wnt signaling pathway to promote its intracellular replication in macrophages. *Frontiers in Immunology* **9**, 1–12.

Wen JJ, Yin YW and Garg NJ (2018) PARP1 depletion improves mitochondrial and heart function in Chagas disease: effects on POLG dependent mtDNA maintenance. *PLoS Pathogens* **14**, 1–24.

Woolsey AM, Sunwoo L, Petersen CA, Brachmann SM, Cantley LC and Burleigh BA (2003) Novel PI 3-kinase-dependent mechanisms of trypanosome invasion and vacuole maturation. *Journal of Cell Science* **116**, 3611–3622.

Xie B, Zhang L, Zhao H, Bai Q, Fan Y, Zhu X, Yu Y, Li R, Liang X, Sun Q, Li M and Qiao J (2018) Poly(ADP-ribose) mediates asymmetric division of mouse oocyte. *Cell Research* **28**, 462–475.

Yang E, Tacchelly-Benites O, Wang Z, Randall MP, Tian A, Benchabane H, Freemantle S, Pikielny C, Tolwinski NS, Lee E and Ahmed Y (2016) Wnt pathway activation by ADP-ribosylation. *Nature Communications* **7**, 11430.

Zhang W, Zhang H, Wang N, Zhao C, Zhang H, Deng F, Wu N, He Y, Chen X, Zhang J, Wen S, Liao Z, Zhang Q, Zhang Z, Liu W, Yan Z, Luu HH, Haydon RC, Zhou L and He TC (2013) Modulation of β-catenin signaling by the inhibitors of MAP kinase, tyrosine kinase, and PI3-kinase pathways. *International Journal of Medical Sciences* **10**, 1888–1898.

https://doi.org/10.1017/S0031182021001402 Published online by Cambridge University Press